Hybrid Laser Arc Welding Process Evaluation on DH36 and EH36 Steel

This study characterizes the effects laser power, arc power, and laser-arc separation have on weld macrostructure, microstructure, and welding arc

BY C. ROEPKE, S. LIU, S. KELLY, AND R. MARTUKANITZ

ABSTRACT

The effects of laser power, arc power, and laser-arc separation on the macrostructure, microstructure, and welding arc were characterized in hybrid laser arc welds on DH36 and EH36 steels. Experiments were done to study a range of arc and laser powers at a constant laser-arc separation and a range of laser powers and laser-arc separation at a constant arc power. High-speed video captured images of the welding in process, and arc voltage and current were also measured. Two distinct weld macrostructure morphologies were observed. The first had a uniform fusion zone, and the second had a two- part fusion zone with an upper laser and arc combined region and a lower laser-only penetration region at the root. This two-part fusion zone was only observed for partial joint penetration welds, and process parameter maps were made to define the windows for both morphologies. Complete penetration welds always exhibited a uniform fusion zone. Decreasing the laser-arc separation increased the total penetration of the uniform fusion zone welds and reduced the size of the laser-only penetration region in the two-part fusion zone welds. The formation of acicular ferrite was promoted by increasing the arc power and increasing the laser-arc separation. Laser power did not have a major effect on the weld metal microstructure. Small laser-arc separations and low laser powers added a low-frequency large globular/short circuiting metal transfer mode to the predominately spray arc. Welding with larger laser-arc separations and higher lasers powers did not exhibit this low-frequency transfer but did have a mid frequency small globular free-flight transfer that was not observed in the gas metal arc welding (GMAW) only arc.

Introduction

Hybrid laser arc welding (HLAW) is a process that combines conventional arc welding, typically gas metal arc welding (GMAW) or gas tungsten arc welding (GTAW), and laser beam welding (LBW) such that both heat sources are incident on a single weld pool (Refs. 1–4). The process was first developed by Steen and Eboo (Ref. 5) using a 2-kW CO_2 laser and GTAW, and it produced some interesting results. The laser was found to stabilize the voltage and current of an unstable arc, reduce the arc column resistance, and increase the depth-to-width ratio of the resulting welding morphology (Ref. 5). As laser technology developed, higher-power welding lasers were more readily available, and the process has gained interest for industrial applications and for research (Refs. 1–4). Hybrid laser arc welding can be divided into the following two general categories: laser-stabilized arc welding (Refs. 6–9) and laser plus arc welding (Refs. 1–4). Laser-stabilized arc welding uses a low-power laser, less than 1 kW and typically around 500 W, such that no keyhole is formed. Here the arc dominates the welding process, although the laser does have some profound effects. The arc voltage is lowered and with reduced fluctuation. Melting efficiency is increased, the arc contracts to a smaller radius, and the cathode spot is fixed to the point of laser incidence (Refs. 6–9). In the laser plus arc welding category, a high-power laser, typically greater than 1 kW, is used so that a keyhole is formed and the arc and laser have similar power levels. Neither power source dominates the welding process. The laser provides improved penetration, and the arc allows root opening bridging ability. In addition, the welding speed is increased over arc welding, and the weld quality is improved over laser beam welding (Refs. 1–4). This research work used a high-power laser and while the process falls into the latter category of laser plus arc welding, the rest of this paper discusses this category of hybrid laser arc welding.

There are many process variables associated with hybrid laser arc welding, and it is important to understand how they affect the welding process. In hybrid laser arc welding, the arc power controls the weld width and root opening bridging ability, and the laser power controls the penetration (Refs. 10–14). Modeling work (Ref. 15) also verifies these results. The laser-arc separation can also be optimized to increase the penetration (Refs. 10, 11); however, laser-arc separation also greatly influences the stability of the process (Refs. 11, 16, 17). Hybrid laser arc welding has an increased melting efficiency, as measured by the weld cross-sectional areas, over the sum of the individual process (Ref. 16). Laser focal position can also influence penetration greatly; it should be slightly below the base metal surface such that the laser is focused on the surface of the depressed weld pool (Refs. 11, 14).

The microstructural development of hybrid laser arc welds is an important research interest. Steel weld metal microstructure depends on the following important parameters: chemical composition, nonmetallic inclusions, solidification structure, prior austenite grain size, and the thermal cycle (Ref. 18). These parameters may be significantly different in hybrid laser arc welds over other more conventional processes and need to be studied in addition to the resultant weld metal microstructure to ensure the viabil-

KEYWORDS

Laser Power
Arc Power
Laser-Arc Separation
Hybrid Laser Arc Welding
DH36 and EH36 Steels

C. ROEPKE and S. LIU (sliu@mines.edu) *are with Center for Welding, Joining and Coatings Research, Colorado School of Mines, Golden, Colo. S. KELLY and R. MARTUKANITZ are with Applied Research Laboratory, Pennsylvania State University, State College, Pa.*

ity of hybrid laser arc welding as an industrial process. The size distribution of nonmetallic inclusions is very important in controlling weld metal microstructure. Acicular ferrite is observed to nucleate on inclusions, and a high content of acicular ferrite is associated with inclusions greater than 0.2 μm, more specifically between 0.4 and 0.6 μm (Refs. 19–21). These inclusions are typically oxides of manganese, aluminum, and titanium, and are formed during deoxidation of the weld pool by the alloy additions of the filler material (Refs. 20, 21). Oxygen potential of the weld system during welding and solidification has an important effect on the type and size of the inclusions that result. Higher oxygen content and short solidification time both promote smaller inclusions (Refs. 19, 22). It is well established in low-carbon structural steel welds that high contents of acicular ferrite generally exhibit high toughness and strength; consequently, acicular ferrite is a preferred weld metal microstructure for good mechanical performance (Refs. 18–22).

There have been several studies focused on the weldment microstructure and mechanical properties of hybrid laser arc welding of steel (Refs. 23–33). Hybrid laser arc welds on DH36 steel using either CO_2 or Nd:YAG lasers with conventional GMAW produced a weld metal microstructure high in acicular ferrite. The hybrid welds also had better weld metal impact toughness, 53 to 64 J at –20°C, than a comparison submerged arc weld (SAW), 49 J at –20°C (Ref. 23). The weld metal hardness of hybrid laser arc welds on DH36 and A36 steel have been reported to be acceptable for arc and laser welding (Refs. 23, 24). Hybrid laser arc welding can be used to weld a variety of pipeline steels (Ref. 26). With the proper filler material that allows for the formation of nonmetallic inclusions, hybrid welds have a predominately acicular ferrite microstructure and acceptable hardness levels. In a higher-alloy steel like HY-80 that has high hardenability, it can be more difficult to produce acicular ferrite in a hybrid laser arc weld because of the high cooling rates and high dilution of the filler material associated with hybrid laser arc welding (Ref. 27). However, through control of heat input and preheat, a predominately acicular ferrite weld metal microstructure can be produced in hybrid laser arc welds on HY-80 (Ref. 28). Because DH36 and EH36 steels do not have as high hardenability as HY-80, it is expected that high contents of acicular ferrite can form in hybrid laser arc welds of these steels. It is also expected that the weld metal microstructure will not be influenced by the change in base material between DH36 and EH36 steels. This is because the chemical compositions of the two steels are very similar (they are designated differently because of different impact toughness requirements), and the weld metal is predominately influenced by the filler material, which remains constant for both base materials. Consequently, DH36 and EH36 steels have been used interchangeably in this study, and no comparison is made between the hybrid laser arc welds made on them.

This research work will have application to the shipbuilding, pipeline, heavy-equipment, and other heavy construction industries. Hybrid laser arc welding allows welding to be done at higher travel speeds, with greater penetration, reduced distortion compared to conventional arc welding (Refs. 34, 35), and improved root opening tolerance over laser beam welding. Understanding the effects of the major hybrid variables on the welding process will be critical to the implementation of hybrid laser arc welding in these industries.

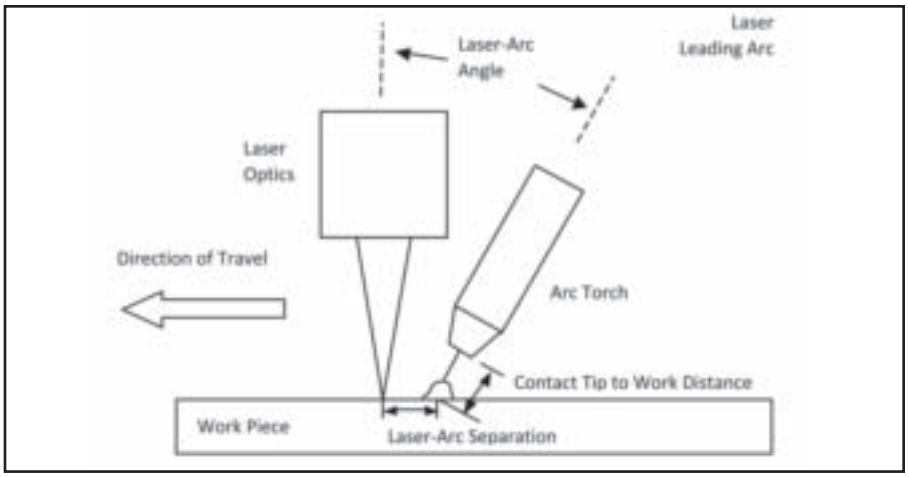

Fig. 1 — Schematic representation of the hybrid laser arc welding setup showing the direction of travel and critical dimensions.

Research Objectives

The main objective of this research was to characterize the effects of the following major hybrid laser arc welding parameters: laser power, arc power, and laser-arc separation on the macrostructure, microstructure, and the welding arc.

Experimental Procedures

The hybrid laser arc welding system consisted of a continuous-wave 14-kW CO_2 laser with an F/# (ratio of raw beam diameter to focal length) of 5.2 and a focused beam diameter of 0.8 mm, and a constant voltage gas metal arc welding power source. The electrode was 0.045-in.- (1.1-mm-) diameter ER70S-6 wire, fed using a conventional wire feeder and GMAW gun. The shielding gas used was 50%He-45%Ar-5%CO_2 (after the work of A. Fellman and V. Kujanpaa (Ref. 36)) and was fed solely through the GMAW gun. Two different base materials were used, 5-mm-thick ABS Grade DH36 steel for welds made with laser powers of 4 and

Table 1 — Measured Base Material Chemical Composition as Determined by Direct Reading Atomic Spectroscopy (wt-%)

Material	C	Mn	Si	P	S	Al	Nb	V	Ti	Cu	Cr	Ni	Mo	Fe	Carbon Equivalent
DH36	0.06	1.39	0.19	0.011	0.004	0.025	0.01[a]	0.06	0.01	0.25	0.11	0.14	0.03	bal	0.39
EH36	0.06	1.38	0.25	0.010	0.004	0.024	0.04	0.05	0.02	0.02	0.02	0.02	0.01	bal	0.35

(a) Under minimum specification requirement of 0.02%.

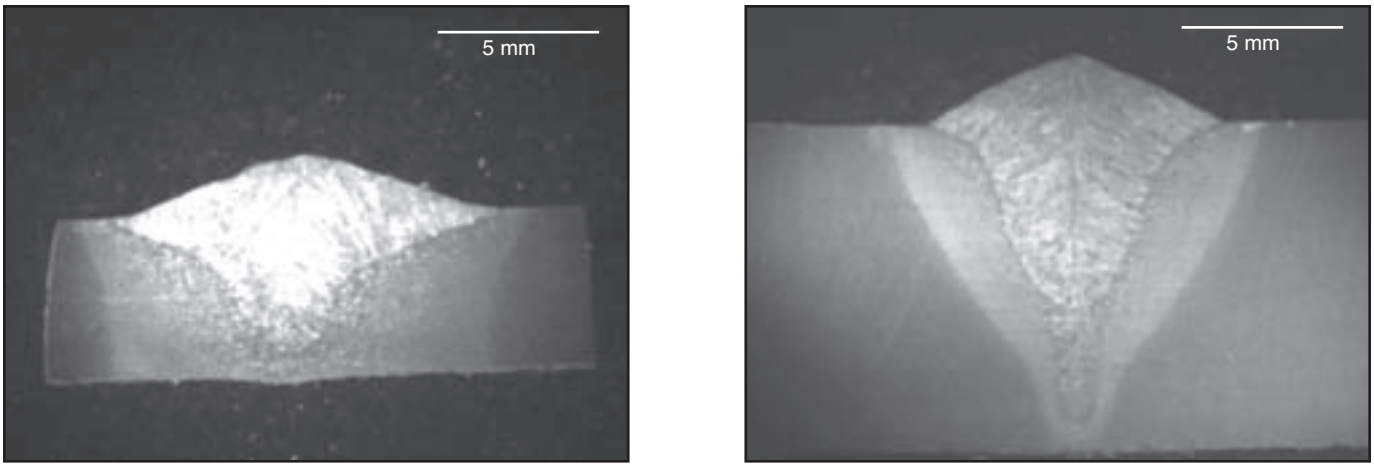

Fig. 2 — Example macrographs of the two distinct morphologies observed in the partial joint penetration welds. Left — Hybrid weld with a uniform fusion zone. Right — Hybrid weld with a two-part fusion zone consisting of an upper, laser, and arc penetration region and a lower, laser-only penetration region.

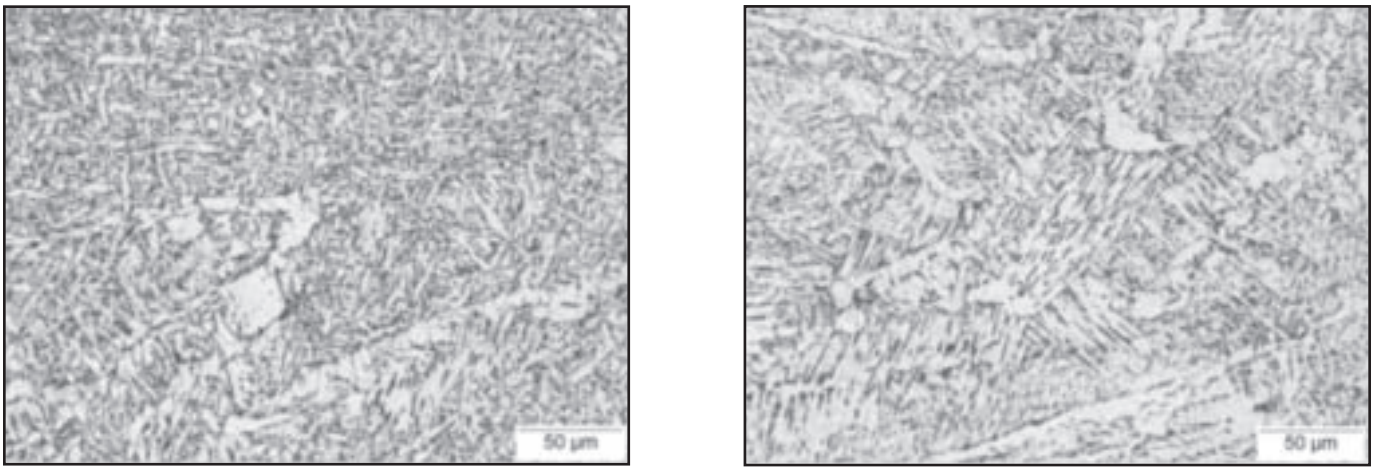

Fig. 3 — Micrographs from a partial-penetration hybrid weld with a two-part fusion zone. Left — Micrograph from the laser and arc penetration region. Right — Micrograph from the laser-only penetration region.

6 kW, and 10-mm-thick ABS Grade EH36 steel for welds made with laser powers of 8 and 9 kW (note the steel grade here is specified in the commercial standard ASTM A131, *Standard Specification for Structural Steel for Ships*). The chemical compositions of these steels are given in Table 1. The reason for selecting the two thicknesses was the need for a thicker material to prevent melt-through at the higher laser powers. At the time of the experiment, only DH36 steel was available in 5 mm thickness and EH36 steel in 10 mm thickness. The base material was cut into 5 cm × 30 cm coupons, and bead-on-plate welds were made. Welding was done with the laser leading the arc. Contact tip-to-work distance and welding angles were all held constant throughout the experiment as shown — Fig. 1. All the constant processing parameters are shown in Table 2.

Table 2 — HLAW Processing Constants

Welding Position	Flat
Process Orientation	Laser leading arc
Laser Focus	At workpiece surface
Laser Orientation	Perpendicular to work
GMAW Polarity	DCEP-CW
Contact Tip-to-Work Distance	0.75 in.
Laser-Arc Angle	15 deg (from laser beam)
Shielding Gas	50%He–45%Ar–5%CO_2
Shielding Gas Flow Rate	150 ft^3/h
Electrode	ER70S-6, 0.045 in. diameter
Travel Speed	30 in./min

An experimental matrix was developed to test the following three major hybrid laser arc welding variables: laser power, arc power, and laser-arc separation. The first experimental matrix used a constant laser-arc separation of 4.5 mm and tested three levels of arc power, 3.4, 6.3, and 8.5 kW, plus four levels of laser power, 4, 6, 8, and 9 kW. The three arc parameters were chosen to produce a change in the dominant metal transfer mode. The 3.4-kW parameter (20 V and 170 A with 200 in./min or 85 mm/s wire feed speed (WFS)) produced predominately short circuiting transfer; the 6.3-kW parameter (28 V and 225 A with 250 in./min or 106 mm/s WFS) was predominately globular transfer; and the 8.5-kW parameter (32 V and 265 A with 300 in./min or 127 mm/s WFS) was predominately spray transfer. The second experimental matrix used a constant arc

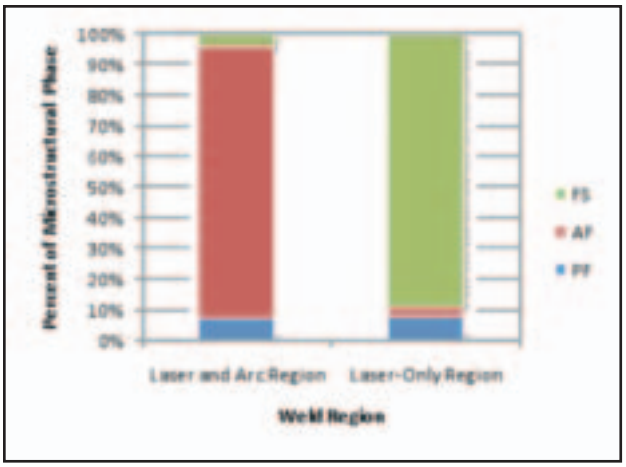

Fig. 4 — Weld metal microstructural content in the two different regions of the two-part fusion zone partial-joint-penetration welds.

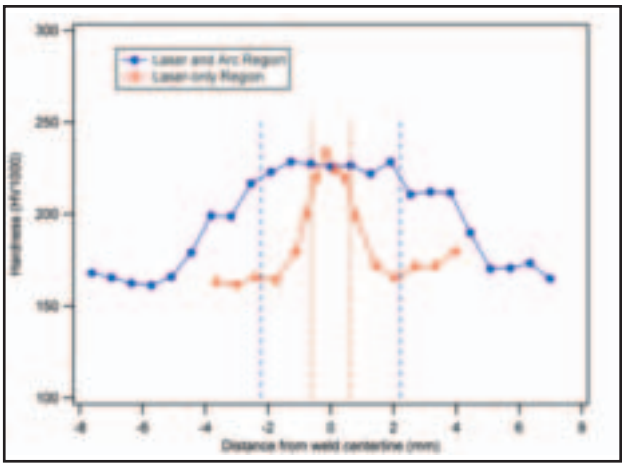

Fig. 5 — Hardness traverses through the two different regions of the two-part fusion zone partial penetration welds. Dotted lines show the location of the weld interface.

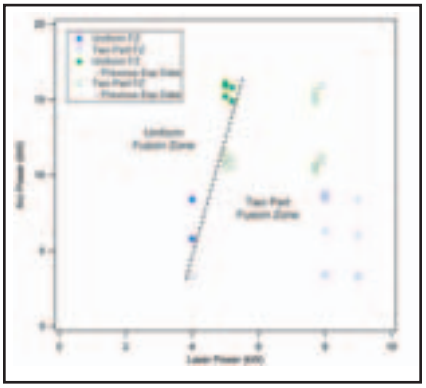

Fig. 6 — Map of the arc power and laser power parameter space for partial-joint-penetration hybrid welding showing the two distinct weld morphologies. The dotted line shows the boundary between the two morphologies. Previous experimental data are from earlier work by the authors that is reported in Ref. 28.

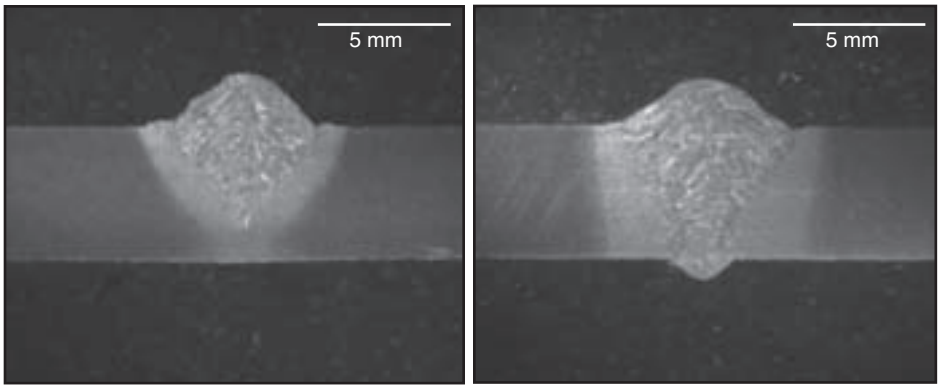

Fig. 7 — Macrographs showing the change in morphology associated with partial and complete penetration welds. Left — Partial penetration weld with a two-part fusion zone made with 4-kW laser power. Right — Full penetration weld with a uniform fusion zone made with 6-kW laser power.

power of 8.5 kW (the spray arc parameter as above) and tested four levels of laser power, 4, 6, 8, and 9 kW, plus four levels of laser-arc separation, 2.0, 4.0, 6.0, and 12.0 mm. In addition to the two matrices, arc-only welds were made at the three arc power levels tested, and laser-only welds were made at the four laser power levels tested.

During welding, a LabVIEW based data-acquisition system was used to monitor arc voltage and current at a 10-kHz sampling rate. Additionally, a high-speed video system was used to capture images of the welding arc, laser plume, and welding pool. The high-speed video camera was filtered with a shade 11 welding lens, and the capture rate was 600 frames/s with an exposure time of 8 μs/frame. The arc voltage and current were analyzed using an IGOR Pro program that computed the average voltage, current, and power, and used a Fast Fourier Transform (FFT) to output the voltage and current frequency spectra. From these frequency spectra, the major voltage and current frequencies could be determined.

Transverse samples for macrostructure and microstructure analysis were sectioned from the center portion of the weld length. The samples were mounted in Bakelite, ground down to 600 grit, and then polished with a diamond suspension down to 1 μm. The welds were etched with a 2% Nital solution for 10 s. Macrographs of the welds were then taken using a stereomicroscope at 10×. The weld morphology was observed, and characterizing dimensions were measured. Multiple micrographs of each of the welds were taken throughout the fusion zone using a light optical microscope at 200×. The weld microstructures were observed and characterized according to the IIW system for the classification of weld metal microstructures (Ref. 37).

Results and Discussion

Macrostructure

When examining the macrostructure of the hybrid laser arc welds, it was immediately apparent that there were two distinct types of morphologies — Fig. 2. The first morphology has a uniform fusion zone (the microstructure is the same everywhere in the fusion zone), much like a conventional gas metal arc weld but with increased penetration. The second morphology has a two-part fusion zone consisting of an upper, laser and arc penetration region (similar to a conventional gas metal arc weld) and a lower, laser-only penetration region (similar to a laser beam weld). This second morphology has been previously observed by

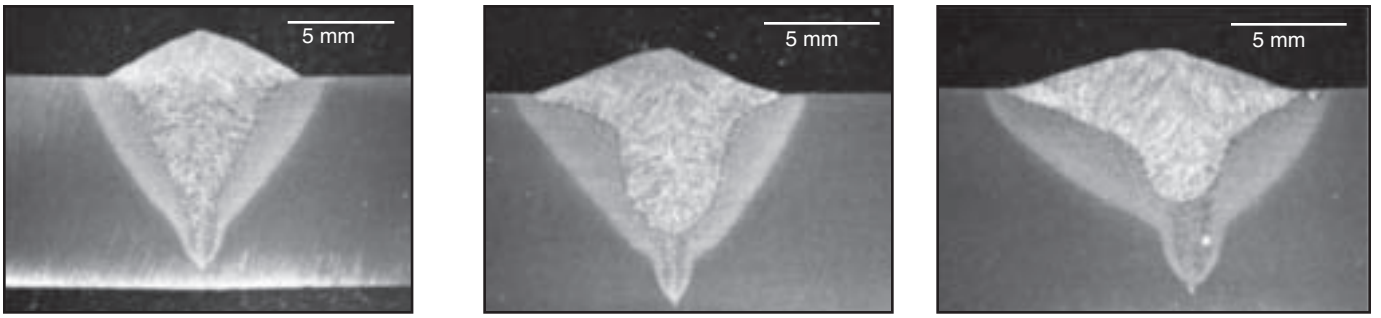

Fig. 8 — Macrographs showing the morphology changes due to the laser-arc separation in the partial penetration welds with a two-part fusion zone. From left, the laser-arc separation is 4.5, 6.0, and 12.0 mm. Laser power and arc power are constant for all welds at 8 and 8.5 kW, respectively.

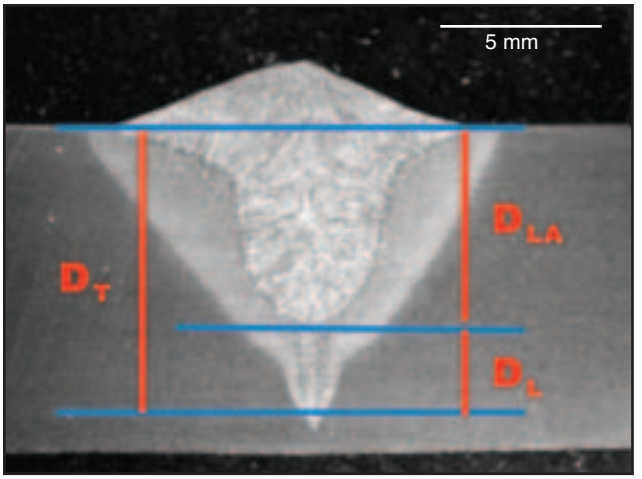

Fig. 9 — Schematic macrograph showing the penetration measurements of the laser and arc region, and the laser-only region.

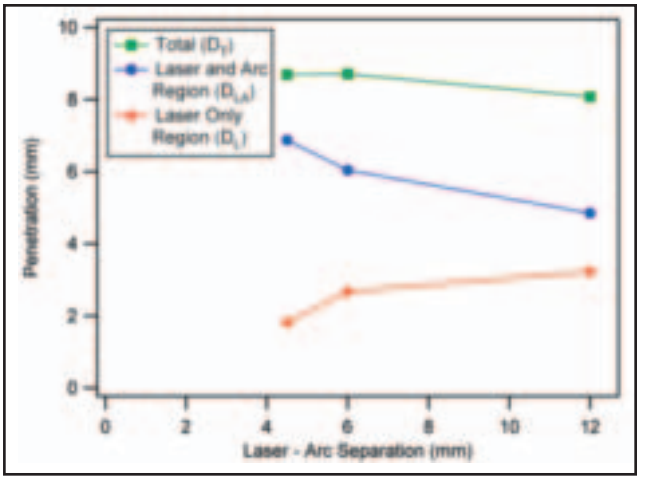

Fig. 10 — Total penetration and the penetration of the two distinct fusion zone regions as a function of the laser-arc separation in-partial penetration bead-on-plate welds. Laser power and arc power are constant for all welds at 8 and 8.5 kW, respectively.

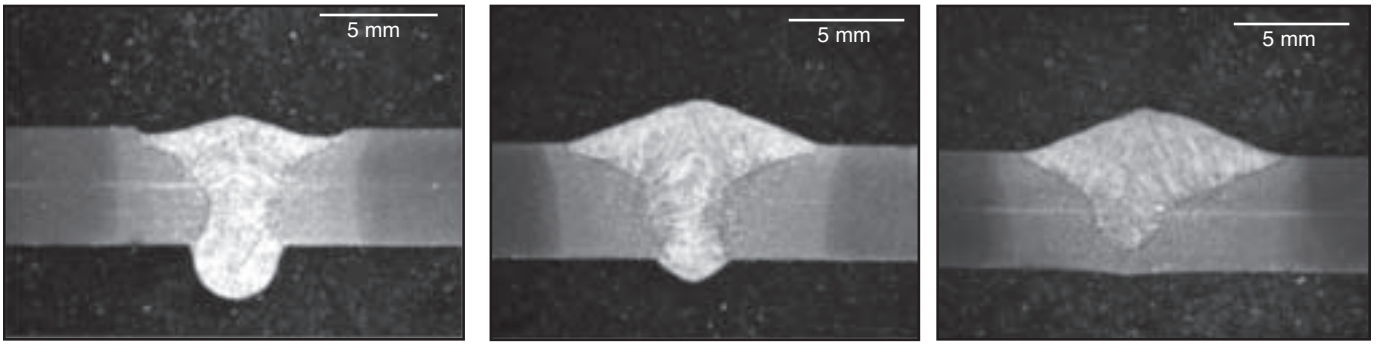

Fig. 11 — Macrographs showing the morphology changes due to the laser-arc separation in the welds with a uniform fusion zone. From left, the laser-arc separation is 4.5, 6.0, and 12.0 mm. Laser power and arc power are constant for all welds at 4 and 8.5 kW, respectively.

the authors (Ref. 28) and by several other researchers (Refs. 29, 30, 33, 38, 39). The two regions in the second morphology not only appeared different at low magnification but also at high magnification. The microstructure of the upper, laser, and arc penetration region is mostly acicular ferrite with some grain boundary ferrite whereas the lower, laser-only penetration region is mostly ferrite with second phases and only a small amount of acicular ferrite — Figs. 3, 4. These differences were also reported by other researchers (Refs. 29, 30). It is likely that this second morphology is the result of incomplete mixing of the filler material from the gas metal arc welding part of the hybrid process to the root of the weldment. The lower, laser-only penetration region is basically an autogenous laser beam weld in the base material. In addition, the lower, laser-only penetration region may actually be solidifying before mixing can occur because of high cooling rates at the root of the weldment. Real-time X-ray transmission imaging of hybrid laser arc welding with tungsten tracers by Naito et al. (Ref. 39) has shown a dual-flow convection pattern in welds with a 5-mm laser-arc separation that would produce this second type of morphology. This dual-flow convection pattern consists of one flow from the bottom of the keyhole up along its sides and another from the center of the arc at the surface down and

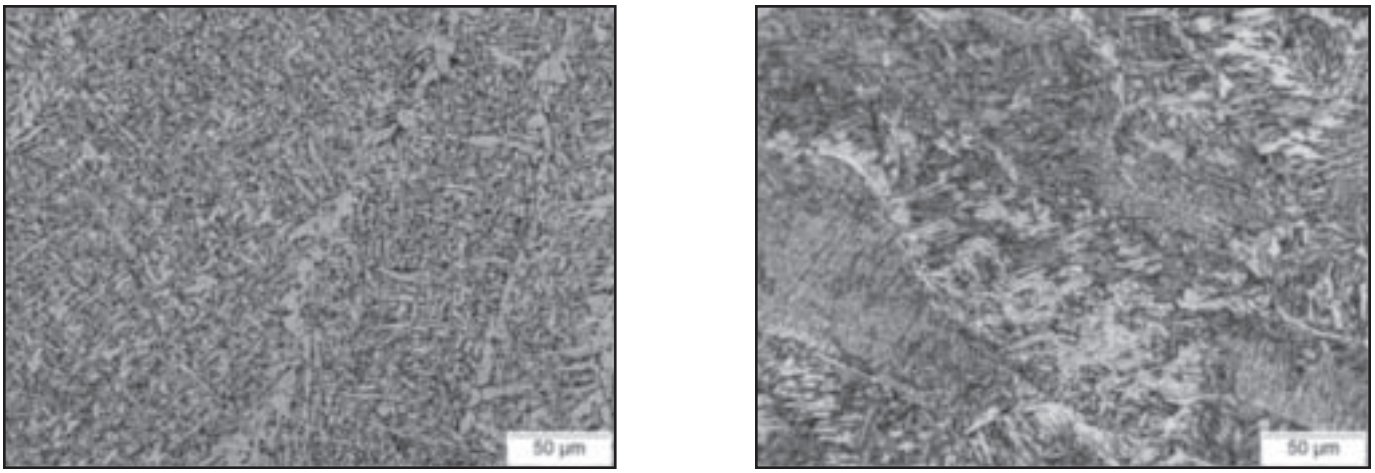

Fig. 12 — Micrographs of the GMAW 8.5-kW arc power, left, and LBW 8-kW laser power, right, comparison welds.

away from the arc. This creates a region at the bottom of the keyhole that flow from the arc never reaches. In general, for hybrid laser arc welding, this second morphology would be undesirable because it has a region that is unalloyed by the filler material from the gas metal arc welding part of the process, and the alloying addition from the gas metal arc welding component is a key advantage of the hybrid laser arc welding process. Hardness traverses measured across both regions show no major difference in weld metal hardness between the two regions — Fig. 5. This behavior is expected because DH36 and EH36 steels both have low hardenability. However, if this morphology were present in a more hardenable steel, it is likely that the laser-only penetration region would have a much higher hardness than the laser and arc penetration region, and this would be undesirable. Much of the rest of this macrostructure discussion focuses on how to eliminate or avoid this laser-only penetration region that creates the second type of fusion zone morphology. A process map laser power and arc power at a laser-arc separation of 6mm was developrd to show the processing windows where the two different morphologies would result — Fig. 6. The figure shown includes data from previous work by authors (Ref. 28), which help define the boundary between the two morphologies. Low laser powers and high arc powers promoted a uniform fusion zone, the first morphology. Welds made with a high lser power and low arc power will have a two-part fusion zone, the second morphology. Work done by Gao et. al. (Ref. 33) also shows that increasing the arc power promotes the uniform fusion zone. It is important to note that this process map was made for partial-penetration welds.

Complete-joint-penetration welds were always observed to have a uniform fusion zone, the first morphology. The microstructure in these complete penetration welds was the same throughout the fusion zone. However, it is possible that there may be some small compositional changes in the fusion zone of these welds; the fluctuation in weld metal composition has not been measured and will be the subject of future work by the authors. Even when a complete penetration weld was achieved by increasing the laser power, such that the weld would now fall in the processing window for the two-part fusion zone morphology as defined on the previous map, a uniform fusion zone was observed. This is believed to be due to the base metal being sufficiently thin to result in complete penetration and partially altering the flow characteristics. This is illustrated in Fig. 7. It is likely that the fluid flow in a complete penetration weld promotes better mixing in the fusion zone and consequently does not have the laser-only penetration region. Additionally, a complete penetration weld changes the heat flow conditions of the weld and, as a consequence, the cooling rate at the root of the weldment will be much slower than in a partial-penetration weld allowing more time for mixing to occur to the root of the weld before solidification. When making complete penetration hybrid laser arc welds, the two-part fusion zone morphology with a laser and arc upper penetration region and a lower laser-only penetration region was not observed.

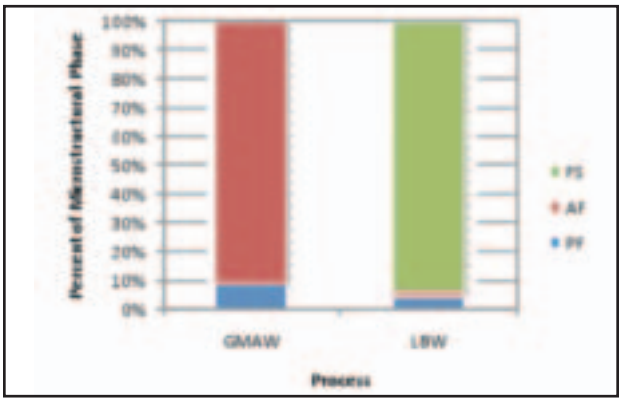

Fig. 13 — Weld metal microstructural content as process. The GMA weld was made with 8.5 kW of arc power, and the laser beam weld was made with 8 kW of laser power.

The laser-arc separation also plays a major role in modifying the hybrid laser arc weld morphology. Considering partial-penetration welds made with 8 kW of laser power and 8.5 kW of arc power as shown in the macrographs, decreasing the laser-arc separation decreased the weld width and reduced the size of the laser-only penetration region — Fig. 8. It may be advantageous to quantitatively describe the changes in the size of the two fusion zone regions as a function of the processing conditions. To do this, the penetration of the laser and arc region, D_{LA}, the penetration of the laser-only region, D_L, and the total penetration, D_T, are defined, and these penetrations are plotted — Figs. 9, 10. The total penetration remained relatively constant over the range of laser-arc separation tested. The penetration of the laser and arc region increased with decreasing laser-arc separation, resulting in a smaller laser-only penetration region. As the spatial separation of the heat sources is reduced, the thermal gradient behind the laser keyhole is also reduced. Consequently, the solidification rate behind the laser keyhole is reduced, allowing greater time for weld metal mixing. It is also likely that the fluid flow pattern in the molten weld pool changes with changing

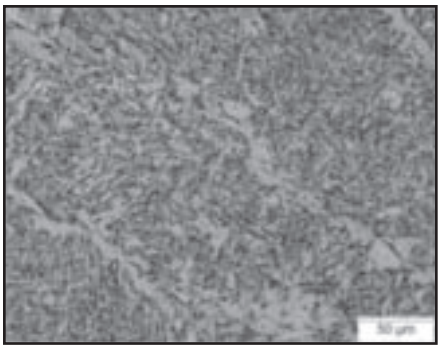

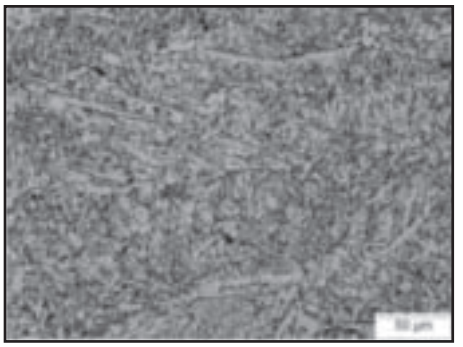

zFig. 14 — Micrographs showing the effect of laser power. From left, the laser power is 4 and 8 kW. Constants include arc power, 8.5 kW, and laser-arc separation, 4.5 mm.

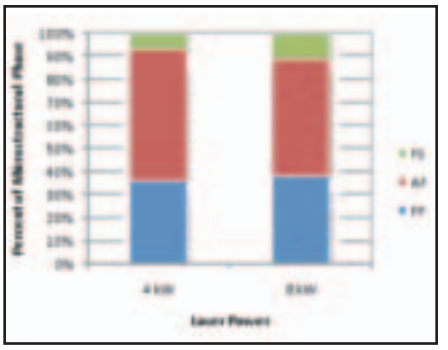

Fig. 15 — Weld metal microstructural content as a function of laser power. Arc power and laser-arc separation were constant at 8.5 kW and 4.5 mm, respectively.

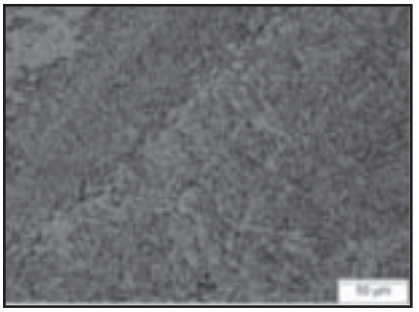

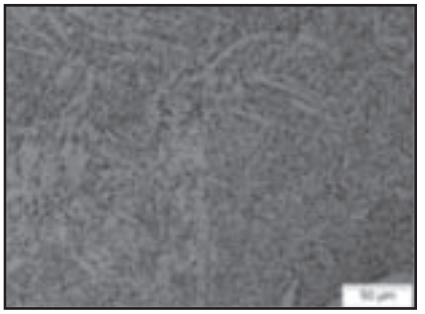

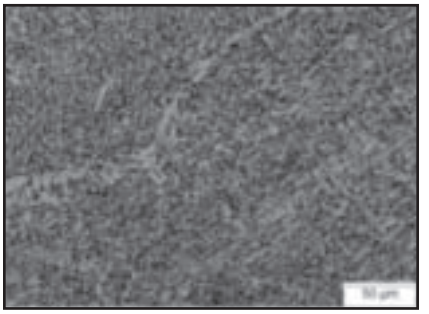

Fig. 16 — Micrographs showing the effect of arc power. From left, the arc power is 3.4, 6.3, and 8.5 kW. Constants include laser power, 8.0 kW, and laser-arc separation, 4.0 mm.

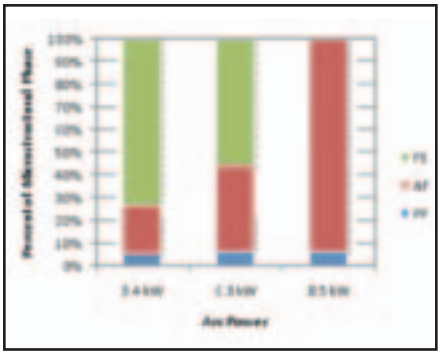

Fig. 17 — Weld metal microstructural content as a function of arc power. Laser power and laser-arc separation were constant at 8.0 kW and 4.0 mm, respectively.

laser-arc separation (Ref. 39), and this may also contribute to the reduced fraction of laser-only penetration. While the fraction of laser-only penetration was reduced by decreasing the laser-arc separation, it was not completely eliminated in the range of laser-arc separation (4.5–12.0 mm) and plate thickness (10 mm) tested. However, extrapolation of the graph shows that it may be possible to produce the uniform fusion zone morphology with no laser-only penetration region if the laser-arc separation is less than 2.0 mm. Consequently, laser-arc separation would be a third variable in creating a boundary on the process map for partial penetration uniform fusion zone welds.

Laser-arc separation also plays a significant factor in hybrid welds with a uniform fusion zone. Figure 11 shows macrographs of welds made with 4 kW of laser power and 8.5 kW of arc power; these parameters produced welds with a uniform fusion zone. Decreasing the laser-arc separation dramatically increased the penetration of these welds. There is also a corresponding decrease in width as laser-arc separation is decreased. From these results, it is clear that reducing the laser-arc separation is advantageous because it promotes higher penetration in the uniform fusion zone welds and reduces the size of the laser-only region in the two-part fusion zone welds.

Microstructure

For microstructural comparison to the hybrid laser arc welds, representative micrographs from a GMA weld made with 8.5-kW arc power and a LBW weld made with 8-kW laser power are provided — Fig. 12. The microstructural content of these welds is shown in Fig. 13. The microstructure of the GMA weld is predominantly acicular ferrite (AF) with a small amount of primary ferrite (PF). The microstructure of the laser beam weld is predominately ferrite with second phases (FS) and a small amount of acicular ferrite (AF) and primary ferrite (PF).

First, the effect of laser power on the microstructure of hybrid laser arc welds in the laser and arc region was examined. Figure 14 shows representative micrographs of the hybrid laser arc welds made with 4 and 8 kW of laser power with constant arc power, 8.5 kW, and constant laser-arc separation, 4.5 mm. The welds had very similar microstructures. The microstructural content of these welds is shown in Fig. 15. The hybrid laser arc weld made with 4 kW of laser power was predominantly acicular ferrite (AF) with a significant amount of primary ferrite (PF) and some ferrite with second phases (FS). The hybrid laser arc weld made with 8 kW of laser power was predominantly acicular ferrite (AF) with a significant amount of primary ferrite (PF) and some ferrite with second phases (FS). The change in laser power from 4 to 8 kW did not produce any major changes in the microstructure of the hybrid laser arc welds. This observation is likely because the major factor in controlling weld metal microstructure is the filler material added, and this did not change when changing laser power.

Next, the effect of arc power on the microstructure of hybrid laser arc welds was examined. Figure 16 shows representative micrographs of the hybrid laser arc welds made with 3.4, 6.3, and 8.5 kW of arc power with constant laser power, 8.0 kW, and constant laser-arc separation, 4.0 mm.

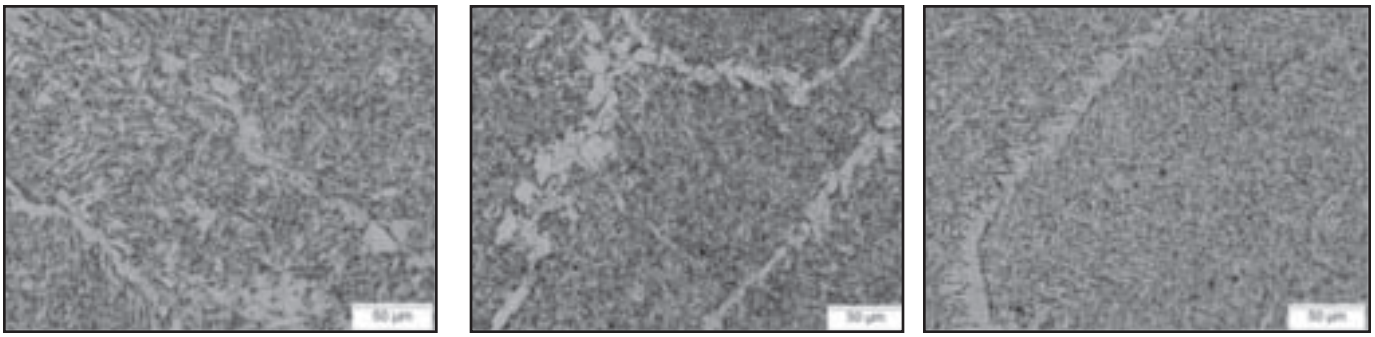

Fig. 18 — Micrographs showing the effect of laser-arc separation. From left, the laser arc separation is 4.5, 6.0, and 12.0 mm. Constants include laser power, 4.0 kW, and arc power, 8.5 kW.

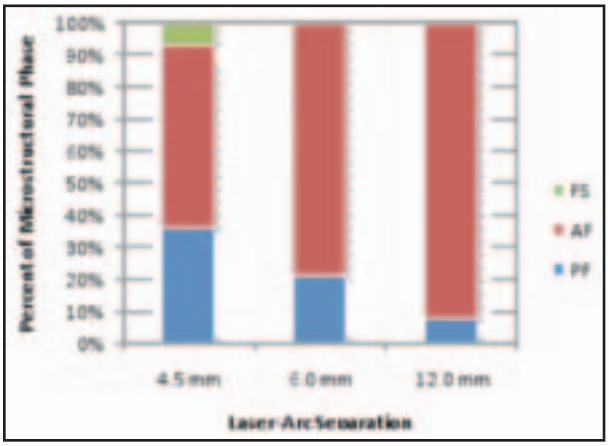

Fig. 19 — Weld metal microstructural content as a function of laser-arc separation. Laser power and arc power were constant at 4.0 and 8.5 kW, respectively.

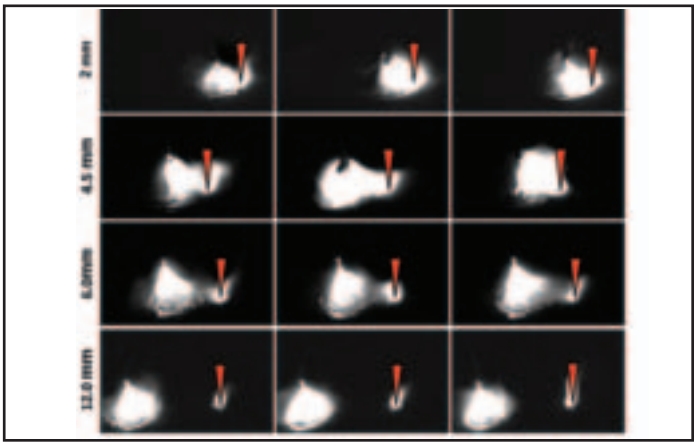

Fig. 20 — Selected high-speed video frames showing the differences caused by changing the laser-arc separation. Red triangles indicate the position of the laser beam.

The microstructural content of these welds is shown in Fig. 17. The hybrid laser arc weld made with 3.4 kW of arc power was predominantly ferrite with second phases (FS) with some acicular ferrite (AF) and a small amount of primary ferrite (PF). The hybrid laser arc weld made with 6.3 kW of arc power was mostly ferrite with second phases (FS) with a significant amount of acicular ferrite (AF) and a small amount of primary ferrite (PF). The hybrid laser arc weld made with 8.5 kW of arc power was predominantly acicular ferrite (AF) and a small amount of primary ferrite (PF). The change in arc power produced significant changes in the microstructure of the hybrid laser arc welds. Increasing the arc power increased the amount of acicular ferrite and decreased the amount of ferrite with second phases. This observation is likely because increasing the arc power increases the total heat input of the process, and the arc power is increased by increasing the wire feed speed, which adds additional filler metal to the weld pool. Both of these effects of increasing the arc power would cause a decrease in the amount of ferrite with second phases and an increase in acicular ferrite. It is also important to note that the filler wire used has been designed to produce a high content of acicular ferrite in conventional GMAW. Because HLAW has increased penetration over GMAW, there is higher base metal dilution in HLAW. This may require higher wire feed rates to be used to counteract the increased penetration in HLAW or new filler wires to be designed specifically for HLAW.

Finally, the effect of laser-arc separation on the microstructure of hybrid laser arc welds was examined. Figure 18 shows representative micrographs of the hybrid laser arc welds made with 4.5, 6.0, and 12.0 mm of laser-arc separation with constant laser power, 4.0 kW, and constant arc power, 8.5 kW. The microstructural content of these welds is shown in Fig. 19. The hybrid laser arc weld made with 4.5 mm of laser-arc separation was predominantly acicular ferrite (AF) with a significant amount of primary ferrite (PF) and some ferrite with second phases (FS). The hybrid laser arc weld made with 6.0 mm of laser-arc separation was predominantly acicular ferrite (AF) and a small amount of primary ferrite (PF). The hybrid laser arc weld made with 12.0 mm of laser-arc separation was predominantly acicular ferrite (AF) and a small amount of primary ferrite (PF). The change in laser-arc separation produced significant changes in the microstructure of the hybrid laser arc welds. Increasing the laser-arc separation increased the amount of acicular ferrite in the welds and promoted a microstructure very similar to the GMAW comparison weld. This is likely because increasing the laser-arc separation decreased the penetration and consequently decreased the dilution of the welding wire.

Welding Arc

The welding arc was observed with high-speed video, and the arc current and voltage were monitored to look for changes in the properties of the arc that may have been caused by the three major hybrid laser arc welding variables. When the arc power was increased in the hybrid laser arc welding process the arc current increased, the predominate frequency in

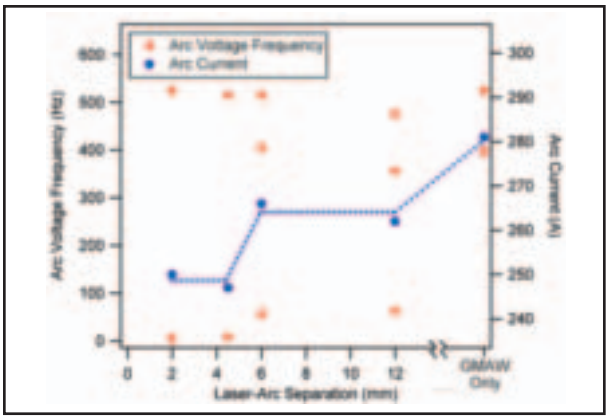

Fig. 21 — Major arc voltage frequencies and corresponding arc current as a function of laser-arc separation.

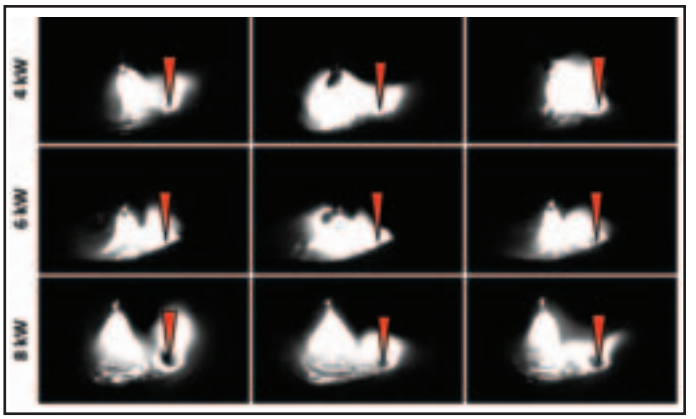

Fig. 22 — Selected high-speed video frames showing the differences caused by changing the laser power. Red triangles indicate the position of the laser beam.

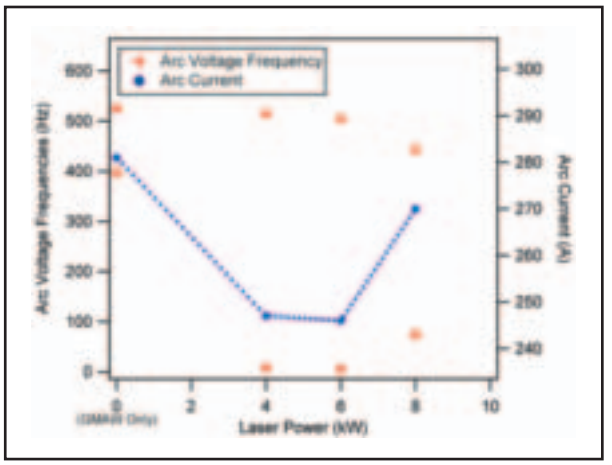

Fig. 23 — Major arc voltage frequencies and corresponding arc current as a function of laser power.

the arc voltage FFT spectrum increased (~10 Hz to ~70 Hz to ~400 Hz and ~525 Hz), and the metal transfer in the arc changed from short circuiting to globular to spray. This behavior is no different than the typical response to changes in arc power in conventional GMAW. Consequently, the discussion focuses only on the effect of laser-arc separation and laser power on the welding arc.

To examine the effect of laser-arc separation on the welding arc, welds were made using an arc power of 8.5 kW; this parameter produced pure spray transfer and a laser power of 4 kW. Figure 20 shows selected high-speed video frames highlighting the differences in the arc caused by laser-arc separation. At 2 mm of laser-arc separation, the arc plasma and laser plasma ejected from the keyhole were nearly always joined. The arc exhibits mostly spray metal transfer; however, there was a low frequency (approximately ten times a second) of large metal globule formation on the tip of the electrode and subsequent violent transfer that sometimes shorted out the arc. It is possible that because of the close proximity of the arc to the laser plasma, the laser plasma is heating the electrode and causing the globule formation. When the laser-arc separation was increased to 4.5 mm the arc behavior was very similar, predominately spray transfer with some low frequency (approximately ten times a second) globular formation and violent transfer. At 4.5 mm, the arc plasma and laser plasma were observed to separate occasionally; however, they were most often joined. Several other researchers (Refs. 11, 16, 17) have shown that small laser-arc separations destabilize the process and increasing the separation stabilizes the process. At 6.0 mm of laser-arc separation, the arc began to behave differently. The arc and laser plasmas were now very infrequently joined, and the arc had a much more stable spray metal transfer with no violent globular/short circuiting transfers. The arc, however, did not have a pure spray metal transfer as some small metal globules were observed to form on the electrode tip and transfer in free flight through the arc. Very similar arc behavior was observed when the laser-arc separation was increased to 12.0 mm. The arc exhibited predominately spray metal transfer with a small amount of small globular transfer. At this laser-arc separation, the arc and laser plasmas were observed to be completely separate from one another. There was, however, still a single weld pool at this laser-arc separation, and because of this the process was still considered "hybrid" and not "tandem."

The arc voltage and current signals corroborated well with the visual observation of the arc behavior. At the low laser-arc separations, 2.0 and 4.5 mm, a new low-frequency (~10 Hz) peak was observed in the voltage FFT that was not observed in the GMA weld — Fig. 21. This voltage frequency would correspond to the large globular/short circuiting transfer that was observed visually with the high-speed video. When the laser-arc separation was increased to 6.0 and 12.0 mm, this low-frequency peak was no longer observed; however, a new mid-frequency (~70 Hz) peak was observed. This peak likely corresponds to the small globular transfer that was visually observed in the welds at these laser-arc separations. In addition to these voltage frequency changes caused by the laser-arc separation, there was also a change in the arc current — Fig. 21. Increasing the laser-arc separation increased the arc current. However, it did so in a stepwise function that seemed to correlate with the observed changes in the voltage frequency and metal transfer mode. The lowest currents, ~250 A, were associated with the low voltage frequency peak and the large globular/short circuiting transfer, while the mid current levels, ~265 A, were associated with the mid voltage frequency and the small globular transfer. The highest current, 281 A, was only observed in the GMA weld that only exhibited high voltage frequencies and pure spray transfer.

To observe the effect of the laser power on the welding arc, welds were made using an arc power of 8.5 kW, which produced pure spray transfer, and a laser-arc separation of 4.5 mm. Figure 22 shows selected high-speed video frames highlighting the differences in the arc caused by laser power. The arc behavior of the welds made with 4 and 6 kW of laser power was very similar. The arc and laser plasmas were observed to be almost always joined, only separating occasionally. The metal transfer was predominantly spray transfer,

but at both of these low laser powers, the large metal globular formation that violently transferred/short circuited was observed. When the laser power was increased to 8 kW the keyhole was observed to be much larger and more stable, and the ejected laser plasma remained more separate from the arc plasma than with the welds made with lower laser powers. The metal transfer was again predominately spray, but the large globular/short circuiting transfer was not observed, and instead a small globular free flight transfer was detected.

These visual observations of the arc and metal transfer correlated well with the arc voltage and current signals. The relationship between metal transfer, voltage frequency, and current was the same as what was observed in the effect of laser-arc separation even though now the changes were caused by laser power level. The effect of laser power on the major arc voltage frequencies and arc current is shown in Fig. 23. The low laser powers, 4.0 and 6.0 kW, that produced the large globular/short circuiting transfer had a low-frequency (~10 Hz) peak observed in the voltage FFT, and the lowest current levels, ~245 A. Other research work (Ref. 40) has shown that the introduction of the laser beam reduces the arc current. When the laser power was increased to 8.0 kW, the small globular free flight transfer was produced, the mid frequency (~70 Hz) voltage peak replaced the low frequency peak, and the current increased to 270 A. Again, this current was still less than the GMAW current, 281 A, that was associated with only the high frequency voltage peaks and a pure spray transfer.

Conclusions

- Partial-joint-penetration hybrid welds should be made within a processing window, defined by a maximum laser power for a given arc power and laser-arc separation, for a uniform fusion zone to prevent laser-only penetration at the root.
- Complete-joint-penetration hybrid welds always had a uniform fusion zone macrostructure and microstructure regardless of the laser power.
- Decreasing the laser-arc separation increased the penetration of the laser and arc region in the two-part fusion zone welds and increased the total penetration in the uniform fusion zone welds.
- Increasing the arc power and increasing the laser-arc separation both promoted the formation of acicular ferrite in the weld metal microstructure. Changes in laser power did not produce a major change in the weld metal microstructure.
- Small laser-arc separations introduced a low frequency large globular/short circuiting transfer in the arc. Larger laser-arc separations produced a mid frequency small globular free flight transfer.
- Low laser powers produced the large globular/short circuiting transfer in the arc, while high laser powers produced the mid frequency small globular free flight transfer.

Acknowledgments

The authors would like to thank Ed Good at the Applied Research Laboratory, Pennsylvania State University, for his help making the welds, and Scott Mitzner at CSM-CWJCR for his help with the preliminary metallographic work. C. Roepke and S. Liu would also like to thank Matt Johnson and Pat Hochanadel at the Los Alamos National Laboratory for their financial support of the graduate research program at the Colorado School of Mines.

References

1. Tusek, J., and Suban, M. 1999. Hybrid welding with arc and laser beam. *Science and Technology of Welding and Joining* 4(5): 308–311.

2. Dilthey, U., and Wieschemann, A. 2000. Prospects by combining and coupling laser beam and arc welding processes. *Welding in the World* 44(3): 37–46.

3. Bagger, C., and Olsen, F. O. 2005. Review of laser hybrid welding. *Journal of Laser Applications* 17(1): 2–14.

4. Mahrle, A., and Beyer, E. 2006. Hybrid laser beam welding — Classification, characteristics, and applications. *Journal of Laser Applications* 18(3): 169–180.

5. Steen, W. M., and Eboo, M. 1979. Arc augmented laser welding. *Metal Construction* 11(7): 332–335.

6. Hu, B., and den Ouden, G. 2005. Laser induced stabilisation of the welding arc. *Science and Technology of Welding and Joining* 10(1): 76–81.

7. Hu, B., and den Ouden, G. 2005. Synergetic effects of hybrid laser/arc welding. *Science and Technology of Welding and Joining* 10(4): 427–431.

8. Shinn, B. W., Farson, D. F., and Denney, P. E. 2005. Laser stabilisation of arc cathode spots in titanium welding. *Science and Technology of Welding and Joining* 10(4): 475–481.

9. Stute, U., Kling, R., and Hermsdorf, J. 2007. Interaction between electrical arc and Nd:YAG laser radiation. *Cirp Annals-Manufacturing Technology* 56(1): 197–200.

10. Qin, G. L., Lei, Z., and Lin, S. Y. 2007. Effects of Nd:YAG laser plus pulsed MAG arc hybrid welding parameters on its weld shape. *Science and Technology of Welding and Joining* 12(1): 79–86.

11. Campana, G., Fortunato, A., Ascari, A., Tani, G., and Tomesani, L. 2007. The influence of arc transfer mode in hybrid laser-MIG welding. *Journal of Materials Processing Technology* 191(1–3): 111–113.

12. Yao, Y., Wouters, M., Powell, J., Nilsson, K., and Kaplan, A. F. H. 2006. Influence of joint geometry and fit-up gaps on hybrid laser-metal active gas (MAG) welding. *Journal of Laser Applications* 18(4): 283–288.

13. Wieschemann, A., Keller, H., and Dilthey, U. 2001. Development of laser-GMA hybrid- and hydra welding processes for shipbuilding. *Welding in the World* 45(7/8): 10–15.

14. Matsuda, J., Utsumi, A., Katsumura, M., Hamasaki, M., and Nagata, S. 1988. TIG or MIG arc augmented laser welding of thick mild steel plate. *Joining and Materials* 1(1): 31–34.

15. Ribic, B., Rai, R., and DebRoy, T. 2008. Numerical simulation of heat transfer and fluid flow in GTA/laser hybrid welding. *Science and Technology of Welding and Joining* 13(8): 683–693.

16. Gao, M., Zeng, X. Y., and Hu, Q. W. 2006. Effects of welding parameters on melting energy of CO_2 laser-GMA hybrid welding. *Science and Technology of Welding and Joining* 11(5): 517–522.

17. Nakajima, T., Sakurai, S., Miyanagi, N., and Takano, Y. 2002. Radiation phenomena in the groove in laser-arc combination welding. *Welding in the World* 46(Special): 51–61.

18. Grong, O., and Matlock, D. K. 1986. Microstructural development in mild low-alloy steel weld metals. *International Metals Review* 31(1): 27–48.

19. Liu, S., and Olson, D. L. 1986. The role of inclusions in controlling HSLA steel weld microstructures. *Welding Journal* 65(6): 139-s to 149-s.

20. Koseki, T., and Thewlis, G. 2005. Inclusion assisted microstructure control in C-Mn and low alloy steel welds. *Materials Science and Technology* 21(8): 867–879.

21. Liao, F. C., and Liu, S. 1992. Effect of deoxidation sequence on carbon manganese steel weld metal microstructures — Deoxidation sequence has a strong influence on nonmetallic inclusions formation and the subsequent weld refinement. *Welding Journal* 71(3): 94-s to 103-s.

22. Osio, A. S., Liu, S., and Olson, D. L. 1996. The effect of solidification on the formation and growth of inclusions in low carbon steel welds. *Materials Science and Engineering a-Structural Materials Properties Microstructure and Processing* 221(1–2): 122–133.

23. McPherson, N. A., Suarez-Fernandez, N., Moon, D. W., Tan, C. P. H., Lee, C. K., and Baker, T. N. 2005. Laser and laser assisted arc welding processes for DH 36 microalloyed steel ship plate. *Science and Technology of Welding and Joining* 10(4): 460–467.

24. Jokinen, T., Viherva, T., Riikonen, H., and Kujanpaa, V. 2000. Welding of ship structural steel A36 using a Nd:YAG laser and gas-metal arc welding. *Journal of Laser Applications* 12(5): 185–188.

25. Gao, M., Zeng, X. Y., Hu, Q. W., and Yan, J. 2009. Laser-TIG hybrid welding of ultrafine grained steel. *Journal of Materials Processing Technology* 209(2): 785–791.

26. Moore, P. L., Howse, D. S., and Wallach, E. R. 2004. Microstructures and properties of laser/arc hybrid welds and autogenous laser welds in pipeline steels. *Science and Technology of Welding and Joining* 9(4): 314–322.

27. Hyatt, C. V., Magee, K. H., Porter, J. F., Merchant, V. E., and Matthews, J. R. 2001. Laser-assisted gas metal arc welding of 25-mm-thick HY-80 plate. *Welding Journal* 80(7): 163-s to 172-s.

28. Roepke, C., and Liu, S. 2009. Hybrid laser arc welding of HY-80 steel. *Welding Journal* 88(8): 159-s to 167-s.

29. Gao, M., Zeng, X. Y., Yan, J., and Hu, Q. W. 2008. Microstructure characteristics of laser-MIG hybrid welded mild steel. *Applied Surface Science* 254(18): 5715–5721.

30. Liu, Z., Kutsuna, M., and Xu, G. 2006. Microstructure and mechanical properties of CO_2 laser-MAG hybrid weld of high strength steel. *Quarterly Journal of the Japan Welding Society* 24(4): 18–23.

31. Metzbower, E. A., Denney, P. E., Moon, D. W., Feng, C. R., and Lambrakos, S. G. 2003. Thermal analysis and microhardness mapping in hybrid laser welds in a structural steel. In *Thermec'2003, Pts 1–5*.

32. Webster, S., Kristensen, J. K., and Petring, D. 2008. Joining of thick section steels using hybrid laser welding. *Ironmaking & Steelmaking* 35(7): 496–504.

33. Gao, M., Zeng, X. Y., Hu, Q. W., and Yan, J. 2008. Weld microstructure and shape of laser-arc hybrid welding. *Science and Technology of Welding and Joining* 13(2): 106–113.

34. Kelly, S. M., Brown, S. W., Tressler, J. F., Martukanitz, R. P., and Ludwig, M. J. 2009. Using hybrid laser arc welding to reduce distortion in ship panels. *Welding Journal* 88(3): 32–36.

35. Reutzel, E. W., Kelly, S. M., Sullivan, M. J., Huang, T. D., Kvidahl, L., and Martukanitz, R. P. 2008. Hybrid laser-GMA welding for improved affordability. *Journal of Ship Production* 24(2): 72–81.

36. Fellman, A., and Kujanpaa, V. 2006. The effect of shielding gas composition on welding performance and weld properties in hybrid CO_2 laser-gas metal arc welding of carbon manganese steel. *Journal of Laser Applications* 18(1): 12–20.

37. Abson, D., Duncan, A., and Pargeter, R. IIW Doc. No. IX-1533-88. Guide to the light microscope examination of ferritic steel weld metals. *IXJ-123-87 Revision 2*, June 1988.

38. El Rayes, M., Walz, C., and Sepold, G. 2004. The influence of various hybrid welding parameters on bead geometry. *Welding Journal* 83(5): 147-s to 153-s.

39. Naito, Y., Mizutani, M., and Katayama, S. 2006. Effect of oxygen in ambient atmosphere on penetration characteristics in single yttrium-aluminum-garnet laser and hybrid welding. *Journal of Laser Applications* 18(1): 21–27.

40. Travis, D., Dearden, G., Watkins, K. G., Reutzel, E. W., Martukanitz, R. P., and Tressler, J. F. 2004. Sensing for monitoring of the laser-GMAW hybrid welding process. *Proceedings of the 23rd International Congress on Applications of Lasers & Electro-Optics*: 33–40.

An Important Event on Its Way?

Send information on upcoming events to the Welding Journal Dept., 550 NW LeJeune Rd., Miami, FL 33126. Items can also be sent via FAX to (305) 443-7404 or by e-mail to *woodward@aws.org*.

Preparation of Manuscripts for Submission to the *Welding Journal* Research Supplement

All authors should address themselves to the following questions when writing papers for submission to the Welding Research Supplement:

Why was the work done?

What was done?

What was found?

What is the significance of your results?

What are your most important conclusions?

With those questions in mind, most authors can logically organize their material along the following lines, using suitable headings and subheadings to divide the paper.

1) **Abstract.** A concise summary of the major elements of the presentation, not exceeding 200 words, to help the reader decide if the information is for him or her.

2) **Introduction.** A short statement giving relevant background, purpose, and scope to help orient the reader. Do not duplicate the abstract.

3) **Experimental Procedure, Materials, Equipment.**

4) **Results, Discussion.** The facts or data obtained and their evaluation.

5) **Conclusion.** An evaluation and interpretation of your results. Most often, this is what the readers remember.

6) **Acknowledgment, References and Appendix.**

Keep in mind that proper use of terms, abbreviations, and symbols are important considerations in processing a manuscript for publication. For welding terminology, the *Welding Journal* adheres to AWS A3.0:2001, *Standard Welding Terms and Definitions.*

Papers submitted for consideration in the Welding Research Supplement are required to undergo Peer Review before acceptance for publication. Submit an original and one copy (double-spaced, with 1-in. margins on 8 ½ x 11-in. or A4 paper) of the manuscript. A manuscript submission form should accompany the manuscript.

Tables and figures should be separate from the manuscript copy and only high-quality figures will be published. Figures should be original line art or glossy photos. Special instructions are required if figures are submitted by electronic means. To receive complete instructions and the manuscript submission form, please contact the Peer Review Coordinator, Erin Adams, at (305) 443-9353, ext. 275; FAX 305-443-7404; or write to the American Welding Society, 550 NW LeJeune Rd., Miami, FL 33126.